Arabian Journal of Chemistry (2013) **xxx**, xxx–xxx

King Saud University

Arabian Journal of Chemistry

www.ksu.edu.sa
www.sciencedirect.com

ORIGINAL ARTICLE

Adsorptive remediation of Cu(II) and Ni(II) by microwave assisted H_3PO_4 activated carbon

Vinod Kumar Gupta [a,*], **Deepak Pathania** [b], **Shikha Sharma** [c]

[a] *Department of Chemistry, Indian Institute of Technology Roorkee, Rookree 247667, India*
[b] *Department of Chemistry, Shoolini University of Biotechnology and Management Sciences, Solan, Himachal Pradesh 173212, India*
[c] *Department of Higher Education, Shimla, Himachal Pradesh, India*

Received 29 August 2013; accepted 13 November 2013

KEYWORDS

Natural fibers;
Microwave activation;
Adsorption;
Isotherm;
Kinetics

Abstract This work explores the feasibility of natural fibers derived from *Ficus carica* plant as an alternative precursor for the preparation of activated carbon via microwave assisted H_3PO_4 activation. The properties of activated carbon were investigated by scanning electron microscope (SEM) and Fourier transform spectroscopy (FTIR). The operational parameters, chemical impregnation ratio, microwave power and irradiation time on the carbon yield and adsorption capability were investigated. Adsorption performance of Cu(II) and Ni(II) onto activated carbon was investigated as a function of pH, contact time, initial metal ion concentration and temperature. The adsorption capacity of Cu(II) and Ni(II) onto the adsorbent was found to be 23.08 and 18.78 mg/g, respectively. Adsorption of metal ions followed second order kinetics with best fit for Fraundlich adsorption isotherm. The values of thermodynamic parameters such as enthalpy change ($\Delta H°$), entropy change ($\Delta S°$) and free energy change ($\Delta G°$) were evaluated for the adsorption of both the metal ions. Adsorption of metal ions onto activated carbon was spontaneous and endothermic in nature. The results suggested that activated carbon developed from natural fibers successfully improved the metal ions adsorption capacity. On the basis of our findings, the adsorbent could be used as a detoxifying agent for better management of industrial effluents.

1. Introduction

The water pollution due to contamination by heavy metal ions was of high concern worldwide. The main sources of heavy metals are mining, metallurgical, chemical manufacturing, tannery, battery manufacturing industries, fossil fuel, chemical industry etc. (Gao et al., 2007). The presence of copper and nickel metal ions in water bodies, their bioaccumulation, potential toxicity, and adverse health effects were a matter of serious concern for the last few decades (Mousavi et al., 2010; Zhao et al., 2012a). Input of Cu(II) and Ni(II)

* Corresponding author. Tel.: +91 1332285801; fax: +91 1332286202.
E-mail addresses: vinodfcy@gmail.com, vinodfcy@iitr.ernet.in (V.K. Gupta).

Peer review under responsibility of King Saud University.

ELSEVIER Production and hosting by Elsevier

1878-5352 © 2013 King Saud University. Production and hosting by Elsevier B.V. All rights reserved.
http://dx.doi.org/10.1016/j.arabjc.2013.11.006

from the industries, such as ferrous and non-ferrous metal-mineral processing, electroplating, porcelain enameling, copper sulfate manufacturing, battery and accumulator manufacturing, municipal wastes and sewage sludge discharges into freshwater, leaching of antifouling marine paints, wood preservatives into aquatic ecosystems, etc. has been increased sharply during the past century. In aquatic systems, these metal ions interact with numerous inorganic and organic compounds resulting in altered bioavailability and toxicity (Nriagu, 1979; Gupta et al., 2010; Juliana et al., 2013; Mudhoo et al., 2012). These interactions were essential for the understanding of copper and nickel toxicokinetics. Higher concentration of Cu(II) and Ni(II) resulted in carcinogenic, mutagenic reactions and may cause headache, dizziness, sickness and vomiting, chest pain, tightness of the chest, dry cough and shortness of breath, rapid respiration, cyanosis and extreme weakness (Gupta et al., 2012a; NAS, 1977). Hence, it becomes essential to reduce Cu(II) and Ni(II) from industrial wastewater to acceptable levels before discharging it into natural water bodies.

Numerous techniques have been investigated to eliminate the heavy metal ions from wastewater, including chemical reduction/precipitation, ion exchange, membrane separation, adsorption, etc. Adsorption technology is the most promising and widely used method to remove heavy metal ions due to its high efficiency for trace ions, easy handling, economical effectiveness and availability of various adsorbents (Hameed, 2009; Gupta et al., 2009a; Atar et al., 2012). Commercial activated carbons are excellent and versatile adsorbents because of their high inter-particulate surface area, high degree of micro-porosity, and surface chemical reactivity. The adsorption efficiency and cost of activated carbons largely depend on its precursor, activators and the production techniques. The use of relatively expensive and non-renewable precursors such as natural coal and conventional long duration heating production methods are major limitations associated with commercial activated carbon (Jagtoyen and Derbyshire, 1993; Gupta et al., 2009b). Nowadays, research has been focused on the production of activated carbons from cheaper, abundantly available, and renewable precursors. The biological materials (fruit stone and shells, agricultural waste and marine algal biomass, etc.) have been considered as potential precursors for activated carbons because of their abundance and renewable nature (Rao et al., 2006).

However, the natural fibers due to high lingo-cellulosic contents are proved to be efficient precursors for the activated carbon production. Therefore, in the present study focus has been given on the bio-based porous carbon prepared from *Ficus crica* fibers. Microwave assisted phosphoric acid activation of carbon has been carried out for effective adsorption of heavy metal ions. Microwave heating has been widely used in the activation of carbon. It is based on dielectric heating in which energy is absorbed by ions or molecules that are either induced or permanent dipoles. Unlike conventional heating, the energy conversion occurs by two mechanisms: ion conduction and dipole rotation inside particles (Foo and Hameed, 2012; Zhao et al., 2012b). So, the treatment time can be appreciably reduced as a result of microwave heating. Generally, H_3PO_4 acts as a dehydrating catalyst, which can promote decomposition of the cellulosic precursor at a lower heat treatment temperature. Moreover, the presence of H_3PO_4 in the interior of the precursor restricts the tar formation of cross-links and inhibits the shrinkage of the precursor particle by occupying certain substantial volumes resulting in the lower weight loss and higher yield for H_3PO_4 impregnated carbon (Ahmad and Thyodan, 2013).

In this study, an attempt was made for evaluating the viability of microwave radiations for the preparation of activated carbon from *Ficus carica* fiber via H_3PO_4 activation. The functional and surface chemistry of the activated carbon was analyzed using some techniques. The adsorption capacity of the activated carbon was attempted for Cu(II) and Ni(II) removal from the aqueous phase. The effect of various reaction parameters such as solution pH, metal ion concentration, contact time, adsorbent dose, temperature, salinity, and hardness was investigated. Moreover, adsorption equilibrium isotherms, kinetics, and thermodynamic studies were also outlined.

2. Materials and methods

2.1. Materials

All chemicals used were of analytical grade and supplied by Sigma Aldrich, India (purity >99%). All dilutions and washings were carried out using double distilled water. Muffle furnace (SUNVIC, UK) was used to carbonize *F. carica* fibers. The stock solution of Cu(II) was prepared at a concentration of 1000 mg/L from copper sulfate using double distilled water. The pH adjustments were made using 0.1 M NaOH and 0.1 N HCl.

FTIR spectra of the samples were recorded on Perkin–Elmer FTIR spectrophotometer (model 400, USA). Scanning electron microscope (JEOL JSM-6100, Japan) was used to study the surface morphology of the adsorbent. UV–visible spectrophotometer (Shimadzu UV-1601, Japan) was used to record the concentration of the Cu(II) and Ni(II) in the different samples.

2.2. Preparation of F. carica activated carbon (FCAC)

2.2.1. Carbonization of F. carica fiber

F. carica bast was collected and washed with double distilled water to remove the adhered impurities. The bast was sodden into water for 30 days to separate the fibers. The obtained fibers were washed in double distilled water several times and dried in air. The dried samples were carbonized at 500 °C in a muffle furnace for about 5 min. The obtained carbon was leveled as FCC. The carbonization process may be represented as:

$$\textit{Ficus carica}\ \text{fiber} \xrightarrow{500\ ^{\circ}\text{C},5\ \text{min}} \text{Carbon(FCC)} + CO_2 \quad \text{(Carbonization)}$$

2.2.2. Activation process

In this process, 25 g of FCC was treated with 70 ml of phosphoric acid solution (20%) to form slurry. Slurry was placed in a microwave oven for activation. The microwave (MW) input power was selected at 600 W and 5 min of irradiation time. The activated carbon was washed with double distilled water until the pH of the washing solution reached 7. The sample

Please cite this article in press as: Gupta, V.K. et al., Adsorptive remediation of Cu(II) and Ni(II) by microwave assisted H_3PO_4 activated carbon. Arabian Journal of Chemistry (2013), http://dx.doi.org/10.1016/j.arabjc.2013.11.006

was dried at 100 °C to obtain activated carbon (FCAC). The activation process may be represented as:

Ficus carica fiber

$$+ H_2PO_4 \overset{\Delta(MW),5\ min}{\rightarrow} \text{Activated Carbon(FCAC)} \quad \text{(Activation)}$$

2.3. Equilibrium experiments

Equilibrium studies at different metal ions concentrations were investigated using the batch adsorption process as described earlier (Gupta et al., 2013). Batch adsorption studies were conducted in a set of 250 ml glass stopper Erlenmeyer flasks containing appropriate dose (0.5 g) of adsorbent and 100 ml of metal ion solution (50–500 mg/L). This mixture solution was agitated at a speed of 500 rpm in a thermoshaker until the equilibrium was attained. After equilibrium, supernatant was filtered and the equilibrium concentration of Cu(II) and Ni(II) was analyzed, respectively, using UV–visible spectrophotometer (Gopalan et al., 2012; Goyal et. al., 2009). The percentage metal ion removal (R) and the amount of metal ion adsorbed per unit mass of adsorbent 'q_e' (mg/g) were calculated using the following equations:

$$\%R = \frac{C_0 - C_e}{C_0} \times 100 \quad (1)$$

$$q_e = (C_0 - C_e) \times \frac{V}{M} \quad (2)$$

where C_0 and C_e are the initial and equilibrium concentrations of the metal ion solution (mg/L), V is the volume of the solution (L), and M is the mass of the adsorbent used (g). The obtained data were fitted into adsorption isotherms, pseudo-first-order, pseudo-second-order and intraparticle diffusion models. For thermodynamics studies, observations were made under optimized conditions at different temperatures (20–50 °C).

3. Results and discussion

3.1. Characterization of FCAC

3.1.1. Scanning electron microscopy (SEM)

The surface morphologies depicted the uneven porosity and rough surface of *Ficus caica* fiber based carbon. However, uniform porosity with significant number of pores was observed for FCAC. Therefore, activated carbon has more possibilities for adsorption of a large variety of polar and non-polar organic or inorganic compounds from water.

3.1.2. Fourier transformer infrared spectroscopy (FTIR)

Fourier transformer infrared spectroscopy results indicated the complex nature of FCC and FCAC. The broad and intense absorption peak at 3400 cm^{-1} corresponds to –OH groups. The absorption band at 1799.49 cm^{-1} was assigned to C=O stretching vibrations of aldehydes, ketones, lactones and carboxylic groups (Sharma et al., 2013). The absorption peaks

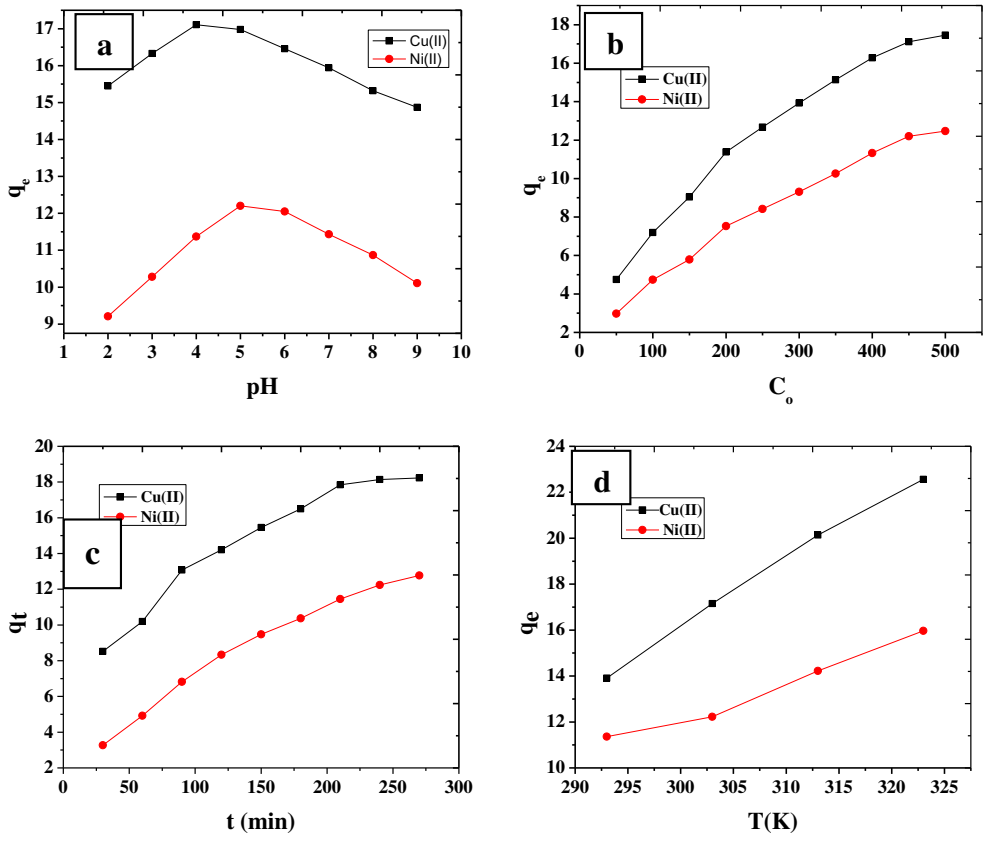

Figure 1 Effect of (a) pH, (b) concentration of metal ion solution, (c) contact time, and (d) temperature on the adsorption of Cu(II) and Ni(II) onto FCAC.

at 1065 and 1415 cm^{-1} may be attributed to vibration of the C═O group in lactones and quinonic groups, respectively (Rosas et al., 2009). The peak at 2922 cm^{-1} may be due to C–H stretching of methyl and methylene groups. These results indicated that FCC contains some amount of quinones that was attributed to the presence of C═O bonds by conjugating with the aromatic rings (Wang and Qin, 2006). It suggested that crosslink reactions together with aromatization have taken place during the carbonization of fibers.

In the case of FCAC, the appearance of additional peaks between 872 and 712 cm^{-1} may be due to the interaction of phosphorous species resulting from phosphoric acid activation (Guo and Rockstraw, 2006). H_3PO_4 may also produce activation through the formation of phosphate and polyphosphate bridges which connect crosslink biopolymer fragments, avoiding the contraction of the material. The removal of the activating agent during washing leads to a matrix in an expanded state with an accessible pore structure (Kennedy et al., 2004).

3.2. Effect of pH

The effect of pH on metal ions adsorption onto FCAC was shown in Fig. 1a. The maximum adsorption of Co(II) and Ni(II) onto the surface of the adsorbent was found to be at pH 4.0 and 5.0, respectively. The association/dissociation of surface functional groups determined the density of surface charge for electrostatic interactions and reactive sites for chemical interactions between the carbon surface and the specific contaminants. It has been observed that adsorption of cationic species depends on the acid oxygen-containing surface functional groups; whereas adsorption of non-ionic or anionic adsorbate species was closely correlated to the surface basicity and oxygen-free Lewis basic sites (Jagtoyen and Derbyshire, 1993).

Depending on the temperature range during carbonization and activation agent of the precursor, oxygen on the carbon surface was present in the form of two types of surface groups: one of which was postulated as carboxyl and lactones evolved on degassing as CO_2 and is acidic in nature. The other oxygen group is quinones, evolved by degassing as CO and is non-acidic in nature (Guo and Rockstraw, 2006). The amounts of these two types of groups depend upon the source of raw material and the history of formation of the activated carbon. Thus, activated carbon may be regarded as being composed of amphoteric solids because of the existence of both negatively and positively charged sites on the surface; which type of sites dominate when activated carbon is placed in aqueous solution depends on the solution pH. In an aqueous solution, the acidic surface oxygen groups undergo ionization producing H^+ ions, the degree of ionization depending on the pH of the solution. This ionization can be shown as:

$$\rangle C - COOH \rightarrow \rangle C - COO^- + H^+$$

$$\rangle C\langle^{COOH}_{COOH} \rightarrow \rangle C\langle^{COO^-}_{COO^-} + 2H^+$$

The H^+ ions are directed toward a liquid phase leaving the carbon surface with negatively charged $-COO^-$ sites. A major fraction of negative sites on the adsorbent was occupied by metal ions via electrostatic attraction in the regions of lower pH. Hence, the maximum metal ion removal was observed at lower pH (Yang et al., 2011). Therefore, the possible mechanisms of metal ion adsorption may be adsorbent–adsorbate electrostatic interactions.

3.3. Effect of initial metal ion concentration

The effect of initial metal ions concentration onto FCAC was shown in Fig. 1b. Adsorption experiments were carried out with varying initial metal ion concentrations from 50 to 500 mg/L using 0.5 g/100 mL activated carbon. The amount of metal ions adsorbed onto activated carbon at equilibrium increased from 4.69 to 17.51 mg/g for Cu(II) and 3.27 to 11.96 mg/g for Ni(II). The increase in uptake capacity of the adsorbent might be due to the fact that the high metal ion concentration provides higher driving force for the transfer process to overcome the mass transfer resistance (Wang et al., 2009; Mittal et al., 2008).

3.4. Effect of contact time

The results of the effect of contact time on the adsorption of Cu(II) and Ni(II) onto FCAC are shown in Fig. 1c. It was revealed that the adsorption of Cu(II) ions onto the adsorbent is relatively faster. The complete adsorption equilibrium between the two phases was obtained after 200 min for Cu(II) and 225 min for Ni(II). The fast metal ions uptakes by the adsorbent was due to their highly porous and mesh like structure, which provided ready access and a large surface area for the adsorption of the metal ions onto the binding sites (Rao et al., 2006).

3.5. Effect of temperature

It has been observed that adsorption of Cu(II) and Ni(II) onto FCAC increased with temperature from 20 to 50 °C (Fig. 1d). It may be due to various factors such as enhancement of interreaction between adsorbent and adsorbate, creation of new adsorption sites and increased rate of intra-particle diffusion at higher temperatures (Srivastava and Tyagi, 1995). The increase in adsorption efficiency with temperature indicated that the reaction follows the endothermic pathway.

3.6. Application of isotherms models

The adsorption data were evaluated in terms of Langmuir, Freundlich, Tempkin, and Dubinin–Radushkevich (DR) isotherm models. The model expressions and linearized forms onto FCAC are shown in Table 1. Each isotherm model describes a particular feature of the adsorption process and a critical analysis of the fitted models was carried out. The value of the isotherms parameters are summarized in Table 2.

Fig. 2a illustrates the Langmuir isotherm for the adsorption of Cu(II) and Ni(II) onto FCAC. The experimental data were analyzed by linear regression analysis and a simple Langmuir isotherm provides an excellent description of the adsorption with correlation coefficients 0.954 for Ni(II) and 0.981 for Cu(II). It has been observed that Cu(II) has a stronger adsorptive potential as its isotherm is located at a lower position in the plot. The values for the Langmuir constant, q_m, have been observed as 23.08 mg/g for copper (II) and 18.78 mg/g for

Please cite this article in press as: Gupta, V.K. et al., Adsorptive remediation of Cu(II) and Ni(II) by microwave assisted H_3PO_4 activated carbon. Arabian Journal of Chemistry (2013), http://dx.doi.org/10.1016/j.arabjc.2013.11.006

Table 1 Expressions for isotherm models and their linearized forms.

Isotherm	Expression	Linearized form	Parameters
Langmuir	$q_e = \frac{q_m K_L C_e}{1+K_L C_e}$	$\frac{1}{q_e} = \frac{1}{q_m} + \frac{1}{K_L q_m C_e}$	K_L, q_m
Freundlich	$q_e = K_F C_e^{1/n}$	$\ln q_e = \ln K_F + \frac{1}{n} \ln C_e$	K_F, n
Dubinin–Radushkevich	$q_e = q_D \exp(-BE^2)$	$\ln q_e = \ln q_D - BE^2$	B, q_D
Temkin	$q_e = \beta \ln(\alpha C_e)$	$q_e = \beta \ln \alpha + \beta \ln C_e$	α, β

Table 2 Isotherm constants and correlation coefficients for the adsorption of Cu(II) and Ni(II) onto FCAC.

Isotherm	Parameters	Cu(II)	Ni(II)
Langmuir	q_m (mg/g)	23.08	18.78
	K_L (L/mg)	0.007	0.004
	R_L	0.237	0.344
	R^2	0.981	0.954
Freundlich	n	2.040	1.736
	K_F (L/g)	0.954	0.384
	R^2	0.995	0.993
Dubinin–Raduskevich	q_D (mg/g)	13.55	9.36
	B (mol^2/kJ^2)	1.29×10^{-4}	2.53×10^{-4}
	E (J/mol)	62.28	44.73
	R^2	0.647	0.673
Tempkin	α (L/g)	0.077	0.046
	β (mg/L)	4.95	3.94
	b	509.41	639.93
	R^2	0.967	0.947

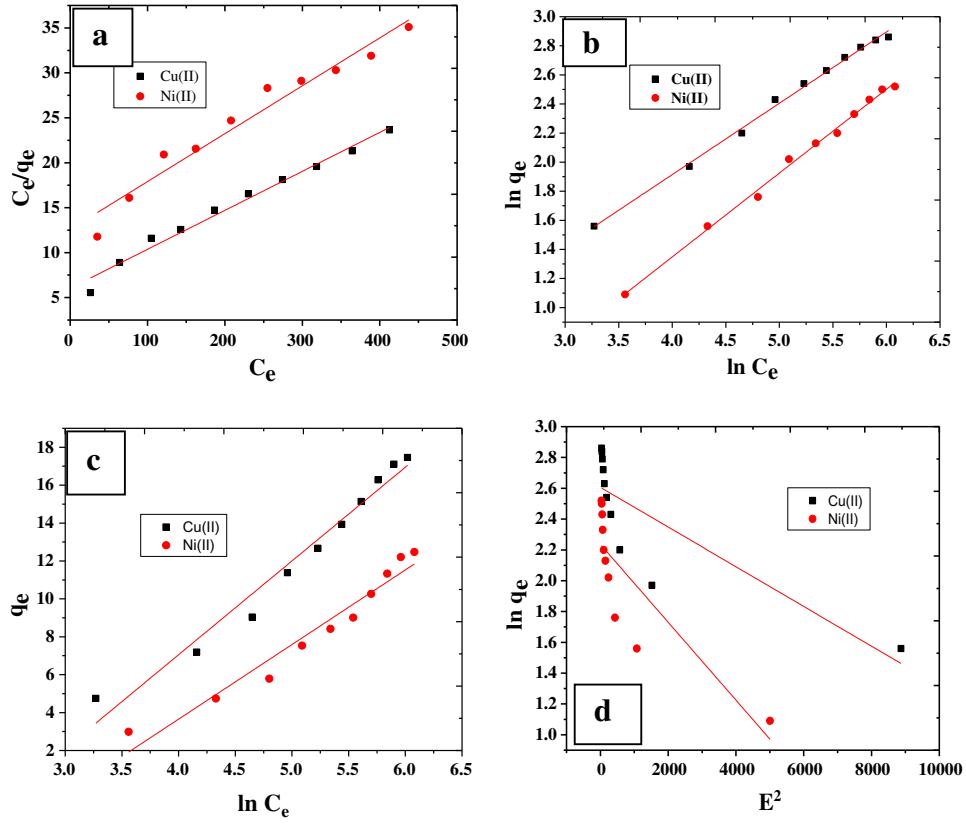

Figure 2 Different isotherms for Cu(II) and Ni(II) adsorption onto FCAC: (a) Langmuir isotherm, (b) Fraundlich isotherm, (c) Dubinin–Radushkevichisotherm, and (d) Temkin isotherm.

Please cite this article in press as: Gupta, V.K. et al., Adsorptive remediation of Cu(II) and Ni(II) by microwave assisted H_3PO_4 activated carbon. Arabian Journal of Chemistry (2013), http://dx.doi.org/10.1016/j.arabjc.2013.11.006

nickel (II). It is perceived by comparison of the results that Cu(II) was removed more extensively than Ni(II) at the optimum pH and temperature. The preference of activated carbon for metal ions has been related to the net effect of metal electronegativity, ionic radius, electrostatic interactions, nature of surface groups, hydration of the ions, etc. (Allen and Brown, 1995; Mittal et al., 2010a).

Freundlich isotherm was commonly used to describe the surface heterogeneity. Fig. 2b depicts the Freundlich isotherm in which constant K_F is related to overall adsorption capacity and constant 'n' is related to surface heterogeneity. The values of isotherm constant (K_F) and coefficient of regression (R^2) are shown in Table 2. The value of n (>1) indicates favorable and heterogeneous adsorption of metal ions onto FCAC (Freundlich, 1906).

The Dubinin–Radushkevich, (R–D) isotherm model (Fig. 2c) was applied to estimate the porosity apparent free energy and the characteristics of sorption (Monika et al., 2009). The estimated constant, B related to adsorption energy of Cu(II) and Ni(II) was presented in Table 2. This constant gives an idea about the mean free energy E, which was valued as 62.28 and 44.73 J/mol for Cu(II) and Ni(II), respectively. E was a parameter used in predicting the type of adsorption (Dubinin, 1960). The E value less than 8 kJ/mol indicated physisorption (Monika et al., 2009). The R–D Theoretical saturation capacity, q_D for Cu(II) and Ni(II) adsorption has been estimated as 13.55 and 9.36 mg/g, respectively.

Tempkin isotherm model assumes that a fall in heat of sorption was linear rather than logarithmic. The data were analyzed according to linear form of the Tempkin model. The isotherm constant α and β are related to maximum binding energy and heat of adsorption, respectively (Fig. 2d).The correlation coefficient values (R^2) and isotherm constants are listed in Table 2.

3.7. Adsorption kinetics

In order to examine the controlling mechanism of the adsorption process, the adsorption data were evaluated in terms of pseudo-first and second-order kinetic models (Pathania and Sharma, 2012). The model expressions and linearized forms are shown in Table 3.

In case of pseudo-first-order rate kinetic equation of Lagergren (1898) the values of the rate constant of adsorption k_1 and adsorption capacity q_e were evaluated from the linear plots of log (q_e–q_t) versus t (Fig. 3a). It was observed that the correlation coefficients R^2 for the linear plots of the pseudo-first order model are 0.977 and 0.942 for Cu(II) and Ni(II), respectively. In the case of pseudo-second-order model (Ho and Mckay, 1999) the values of k_2 and q_e can be determined experimentally from the slope and intercept of a plot of t/q_t versus t (Fig. 3b). It is evident from Table 4 that the correlation coefficients R^2 for the linear plots of the pseudo-second-order model were 0.996 and 0.984 for Cu(II) and Ni(II), respectively. The higher values of R^2 were recorded for the pseudo-second-order compared to pseudo-first-order model. This indicates that the adsorption kinetic was better represented by the pseudo-second-order model for both metal ions. Therefore, the overall rate of the metal ions adsorption process appears to be controlled by the chemical process via ion exchange and/or complexation process (Wang and Qin, 2006).

Table 3 Expressions for kinetics models and linearized forms.

Kinetic Model	Expression	Parameters
Pseudo first order	$\log(q_e - q_t) = \log q_e - \frac{k_1 t}{2.303}$	k_1, q_e
Pseudo second order	$\frac{t}{q_t} = \frac{1}{k_2 q_e^2} + \frac{t}{q_e}$	k_2, q_e
Intraparticle diffusion	$q_t = k_{id} t^{1/2} + C$	k_{id}, C

The intraparticle diffusion model was investigated to identify the adsorption mechanism and to predict the rate controlling step, where C is the intercept and k_{id} (mg/g min$^{1/2}$) is the intraparticle diffusion rate constant which can be evaluated from the intercept and slope of the plot of q_t versus $t^{1/2}$ (Fig. 3c). The intraparticle diffusion model usually includes three steps. The first portion is the external surface adsorption or boundary layer diffusion. The second portion is the gradual stage of adsorption which is the intraparticle diffusion. If the plot of q_t versus $t_{1/2}$ is linear and passes through the origin, then the intraparticle diffusion was the rate-controlling step. The third portion is the final equilibrium stage where the intraparticle diffusion slows down due to the saturation of adsorption sites (Li et al., 2009; Gupta et al., 2011a,b).

Fig. 3c showed that the linear plots did not pass through the origin and indicated that the intraparticle diffusion was not the only rate controlling step and the boundary layer diffusion controlled the adsorption to some degree. This deviation may be due to the difference in the mass transfer rate in the initial and final stages of adsorption. The values of C and k_{id} are given in Table 4. A high value of C in the case of Cu(II) than Ni(II) indicated an increasing boundary layer effect in Cu(II) adsorption onto activated carbon.

3.8. Adsorption thermodynamics

The thermodynamics of adsorption of the adsorbate onto FCAC adsorbent was evaluated from free energy change (ΔG^0), enthalpy change (ΔH^0) and entropy change (ΔS^0) of sorption using the following equations:

$$\ln K_D = -\frac{\Delta G^0}{RT} \quad (3)$$

$$K_D = \frac{C_0 - C_e}{C_e} \quad (4)$$

$$\Delta G^0 = -2.303 RT \log K_D \quad (5)$$

The other thermodynamic parameters such as change in standard enthalpy (ΔH^0) and standard entropy (ΔS^0) were determined using the following equation

$$\Delta G^0 = \Delta H^0 - T\Delta S^0 \quad (6)$$

$$\ln K_D = \frac{\Delta S^\circ}{R} - \frac{\Delta H^\circ}{RT} \quad (7)$$

where, R is universal gas constant (8.314 kJ/mol), C_0 and C_e are the initial and equilibrium concentrations (mg/L). ΔS^0 and ΔH^0 were obtained from the slope and intercept of the vant Hoff's plot of ln K_D versus $1/T$ (Fig. 3d). The thermodynamic parameters for Cu(II) and Ni(II) adsorption onto activated carbon is shown in Table 5. The positive value of ΔH^0 indicated that metal ions adsorption was a physical and

Please cite this article in press as: Gupta, V.K. et al., Adsorptive remediation of Cu(II) and Ni(II) by microwave assisted H_3PO_4 activated carbon. Arabian Journal of Chemistry (2013), http://dx.doi.org/10.1016/j.arabjc.2013.11.006

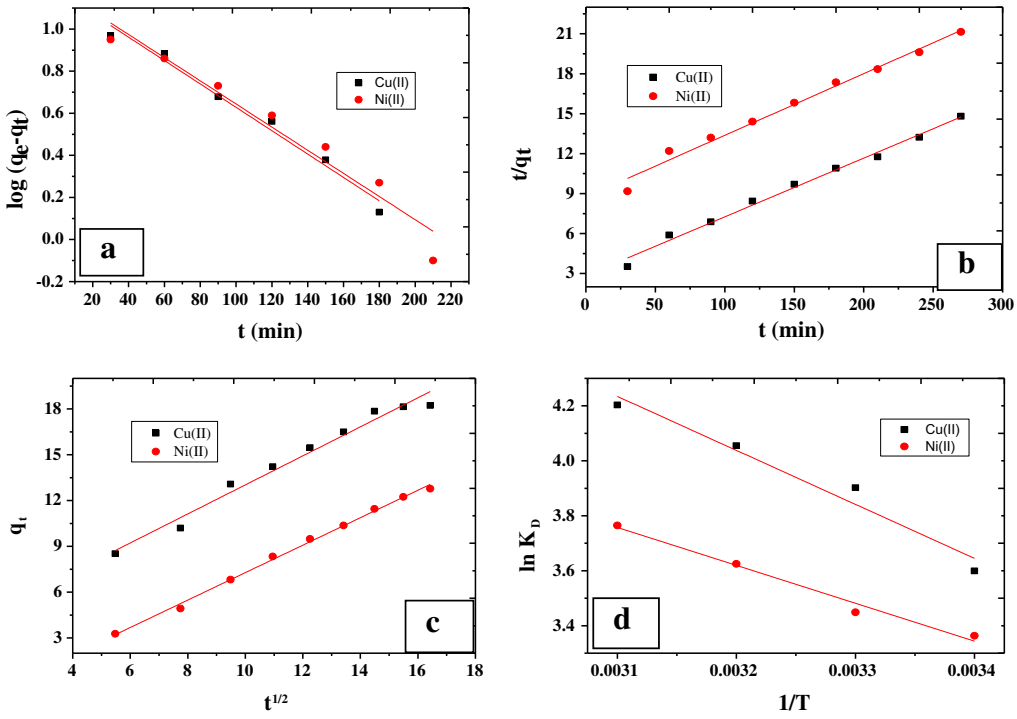

Figure 3 Different plots for Cu(II) and Ni(II) adsorption onto FCAC: (a) pseudo first plot, (b) second order plot, (c) intraparticle diffusion plot, and (d) vant Hoff's plot.

Table 4 Kinetics parameters for the adsorption of Cu(II) and Ni(II) onto FCAC.

Model/parameters	Cu(II)	Ni(II)
Pseudo first order model		
k_1 (min^{-1})	0.013	0.013
q_e (mg/g)	15.24	15.64
R^2	0.977	0.942
Pseudo second order model		
k_2(g mg^{-1} min^{-1}	5.29×10^{-4}	2.45×10^{-4}
q_e (mg/g)	23.92	21.60
R^2	0.996	0.984
Intraparticle diffusion model		
k_{id} (mg/g $min^{1/2}$)	0.951	0.899
C (mg/g)	3.52	1.72
R^2	0.975	0.996

endothermic reaction in both the cases that further confirmed strong interactions between the adsorbate and adsorbent species. An adsorption process is generally considered as physical if $\Delta H^0 < 25$ kJ/mol and as chemical when $\Delta H^0 > 40$ kJ/mol (Gupta et al., 2012b; Mittal et al., 2009). The negative values of ΔG^0 at 20–50 °C of metal ions indicated spontaneous adsorption. Further, the positive value of entropy change, ΔS^0 reflected the increased randomness at the solid–solution interface during the fixation of the adsorbate on the active sites of the adsorbent. This was due to the fact that before the adsorption process starts, the adsorbate ions in solution are heavily solvated and the system is more ordered. The order is lost when the ions were adsorbed on the surface, due to the release of solvated water molecules (Gupta et al., 2001;2002;2003;2005;2006a;2006b). Moreover, the adsorbed solvent (water) molecules which were displaced by the adsorbed species, gain more translation entropy.

3.9. Comparison with other adsorbents

The values of the adsorption capacities (q_m) obtained in this study were 23.08 mg/g for Cu(II) and 18.78 mg/g for Ni(II). The values of q_m for the adsorption of Cu(II) were reported to be 19.50 mg/g for activated carbon from *Phaseolus aureus* hulls (Rao et al., 2009), 81.47 mg/g for tanninimmobilised hydrotalcite (Anirudhan and Suchithra, 2008) and 51.51 mg/g for adsorption onto dehydrated wheat bran (Ozer et al., 2004) and 12.4 mmol/kg for cotton cellulose, 14.6 mmol/kg

Table 5 Thermodynamic parameters for the adsorption of Cu(II) and Ni(II) onto FCAC.

	ΔH^0 (kJ/mol)	ΔS^0 (J/mol K)	ΔG^0 (kJ/mol)			
			293 K	303 K	313 K	323 K
Cu(II)	16.34	85.85	−8.82	−9.68	−10.53	−11.39
Ni(II)	11.47	66.80	−8.10	−8.77	−9.44	−10.11

for sawdust, and 14.8 mmol/kg for short flax fiber (Nikiforova et al., 2010).

The value of nickel(II) uptake was found higher than other reported values in our findings. The values of q_m for the adsorption of Ni(II) were reported to be 7.49 mg/g for groundnut shells and sawdust (Shukla and Pai, 2005), 2.68 mg/g for the modified pine tree materials (Argun et al., 2005), 15.26 mg/g for tea factory waste (Malkoc and Nuhoglu, 2005).

The comparison of adsorption capacity of FCAC used in this study with others found in the literature showed that the activated carbon from the bast fiber was an effective adsorbent for the removal of Cu(II) and Ni(II) from aqueous solution.

4. Conclusions

The activated carbon prepared from natural fiber after activation with phosphoric acid was employed as a potentially low cost adsorbent for the removal of Cu(II) and Ni(II) ions from aqueous solution. Batch adsorption test showed that the extent of metal ion adsorption was dependent on initial concentration, contact time, pH and temperature. The maximum removal of the metal ions was observed at the pH 4.0 for Cu(II) and pH 5.0 for Ni(II). The high values of correlation coefficients indicated that there was a good agreement between the kinetic data of adsorption and the pseudo-second-order model. The adsorption capacity and other parameters were evaluated using Langmuir, Freundlich, Tempkin and Dubinin–Radushkevich isotherm models. The equilibrium data fitted well with the Langmuir model. The monolayer adsorption capacity was found to be 23.08 mg/g for Cu(II) and 18.78 mg/g for Ni(II) at 30 °C. The adsorption capacity of activated carbon for Cu(II) and Ni(II) was found to be relatively high compared with some other adsorbents reported in the literature. The results of the scale-up study may be evidence for the economic detoxification of Cu(II) and Ni(II) from aqueous systems.

References

Ahmad, M.J., Thyodan, S.K., 2013. Microwave assisted preparation of microporous activated carbons from Siris seeds pods for adsorption of metronidazole antibiotic. Chem. Eng. J. 214, 310–318.

Allen, S.J., Brown, P.A., 1995. Isotherm analyses for single component and multi-component metal sorption onto lignite. J. Chem. Technol. Biotechnol. 62, 17–24.

Argun, M.E., Dursun, S., Gur, K., Ozdemir, C., Karatas, M., Dogan, S., 2005. Nickel adsorption on the modified pine tree materials. Environ. Technol. 26, 479–488.

Atar, N., Olgun, A., Wang, S., 2012. Adsorption of cadmium (II) and zinc (II) on boron enrichment process waste in aqueous solutions: batch and fixed-bed system studies. Chem. Eng. J. 192, 1–7.

Dubinin, M.M., 1960. The potential theory of adsorption of gases and vapors for sorbents with energetically non-uniform surface. Chem. Rev. 60, 235–266.

Foo, K.Y., Hameed, B.H., 2012. Preparation of activated carbon by microwave heating of lang sat (Lansium Domesticum) empty fruit bench waste. Bioresour. Technol. 116, 522–525.

Freundlich, H.M.F., 1906. Over the adsorption in solution. J. Phys. Chem. 57, 385–471.

Gao, Hong.-Wen., Chen, Fang.-Fang., Ling, C., Teng, Z., Lu-Ting, P., Jian-Hua, L., Hua-Fei, L., 2007. A novel detection approach based on chromophore-decolorizing with free radical and application to photometric determination of copper with acid chrome dark blue. Anal. Chim. Acta 587, 52–59.

Gopalan, R., Anand, A., Sugumar, W.R., 2012. A Laboratory Manual for Environmental Chemistry. I.K. International Publishing House Pvt. Ltd, New Delhi, India.

Goyal, R.N., Gupta, V.K., Chatterjee, S., 2009. A sensitive voltammetric sensor for determination of synthetic corticosteroid triamcinolone, abused for doping. Biosensors and Bioelectronics 24, 3562–3568.

Guo, Y.P., Rockstraw, D.A., 2006. Physical and chemical properties of carbons synthesized from xylan, cellulose, and kraft lignin by H_3PO_4 activation. Carbon 44, 1464–1475.

Gupta, V.K., Gupta, M., Sharma, S., 2001. Process development for the removal of lead and chromium from aqueous solutions using red mud – an aluminium industry waste. Water Res. 35, 1125–1134.

Gupta, V.K., Chandra, S., Mangla, R., 2002. Dicyclohexano-18-crown-6 as active material in PVC matrix membrane for the fabrication of cadmium selective potentiometric sensor. Electrochimica Acta 47, 1579–1586.

Gupta, V.K., Prasad, R., Kumar, A., 2003. Preparation of ethambutol-copper(II) complex and fabrication of PVC based membrane potentiometric sensor for copper. Talanta 60, 149–160.

Gupta, V.K., Chandra, S., Lang, H., 2005. A highly selective mercury electrode based on a diamine donor ligand. Talanta 66, 575–580.

Gupta, V.K., Jain, A.K., Kumar, P., 2006a. PVC-based membranes of N, N′-dibenzyl-1,4,10,13-tetraoxa-7,16-diazacyclooctadecane as Pb(II)-selective sensor. Sensors and Actuators, B: Chemical 120, 259–265.

Gupta, V.K., Jain, A.K., Maheshwari, G., Lang, H., Ishtaiwi, Z., 2006b. Copper(II)-selective potentiometric sensors based on porphyrins in PVC matrix. Sensors and Actuators, B: Chemical 117, 99–106.

Gupta, V.K., Carrott, P.J.M., Carrott, M.M.L., Suhas, R., 2009a. Low-cost adsorbents: growing approach to wastewater treatment. Review. Crit. Rev. Environ. Sci. Technol. 39, 783–842.

Gupta, V.K., Mittal, A., Malviya, A., Mittal, J., 2009b. Adsorption of carmoisine A from wastewater using waste materials – bottom ash and deoiled soya. J. Colloid Interface Sci. 335, 24–33.

Gupta, V.K., Rastogi, A., Nayak, A., 2010. Biosorption of nickel onto treated alga (Oedogonium hatei): Application of isotherm and kinetic models. J. Colloid Interface Sci. 342, 533–539.

Gupta, V.K., Ali, I., Saleh, T.A., Nayak, A., 2011a. Chromium removal by combining the magnetic properties of iron oxide with adsorption properties of carbon nanotubes. Water Res. 45, 2207–2212.

Gupta, V.K., Jain, R., Radhapyari, K., Jadon, N., Agarwal, S., 2011b. Voltammetric techniques for the assay of pharmaceuticals-A review. Analytical Biochemistry 408, 179–196.

Gupta, V.K., Agarwal, S., Singh, P., Pathania, D., 2012. Acrylic acid grafted cellulosic *luffa cylindrical* fiber for the removal of dye and metal ions. Carbohydr. Polym. 98, 1214–1221.

Gupta, V.K., Pathania, D., Agarwal, S., Sharma, S., 2012. Decolorization of hazardous dye from water system using chemical modified *Ficus carica* adsorbent. J. Mol. Liq. 174, 86–94.

Hameed, B.H., 2009. Evaluation of papaya seed as a nonconventional low cost adsorbent for removal of MB. J. Hazard. Mater. 162, 939–944.

Ho, Y.S., McKay, G., 1999. Pseudo-second-order model for sorption process. Process Biochem. 34, 451–465.

Jagtoyen, M., Derbyshire, F., 1993. Some considerations of the origins of porosity in carbons from chemically activated wood. Carbon 31, 1185–1192.

Izidoro, Juliana C., Fungaro, Denise A., Abbott, Jennifer E., Wang, S., 2013. Synthesis of zeolites X and A from fly ashes for cadmium and zinc removal from aqueous solutions in single and binary ion systems. Fuel 103, 827–834.

Kennedy, L.J., Vijaya, J.J., Sekaran, G., 2004. Effect of two-stage process on the preparation and characterization of porous carbon

Please cite this article in press as: Gupta, V.K. et al., Adsorptive remediation of Cu(II) and Ni(II) by microwave assisted H_3PO_4 activated carbon. Arabian Journal of Chemistry (2013), http://dx.doi.org/10.1016/j.arabjc.2013.11.006

composite from rice husk by phosphoric acid activation. Ind. Eng. Chem. Res. 43, 1832–1839.
Lagergren, S.K., 1898. About the theory of so-called adsorption of soluble substances. Handingarl 24, 1–39.
Li, J., Lin, Q., Zhang, X., Yan, Y., 2009. Kinetic parameters and mechanisms of the batch biosorption of Cr (VI) and Cr(III) onto leersia hexandra swartz biomass. J. Colloid Interface Sci. 333, 71–77.
Malkoc, E., Nuhoglu, Y., 2005. Investigations of nickel(II) removal from aqueous solutions using tea factory waste. J. Hazard. Mater. 127, 120–128.
Mittal, A., Gupta, V.K., Malviya, A., Mittal, J., 2008. Process development for the batch and bulk removal and recovery of a hazardous, water-soluble azo dye (Metanil Yellow) by adsorption over waste materials (Bottom Ash and De-Oiled Soya). J. Hazard. Mater. 151 (2–3), 821–832.
Mittal, A., Mittal, J., Malviya, A., Kaur, D., Gupta, V.K., 2010a. Adsorption of hazardous dye crystal violet from wastewater by waste materials. J. Colloid Interface Sci. 343 (2), 463–473.
Mittal, A., Mittal, J., Malviya, A., Gupta, V.K., 2009. Adsorptive removal of hazardous anionic dye "Congo red" from wastewater using waste materials and recovery by desorption. J. Colloid Interface Sci. 340, 16–26.
Monika, J., Garg, V., Kadirvelu, K., 2009. Chromium (VI) removal from aqueous solution, using sunflower stem waste. J. Hazard. Mater. 162, 365–372.
Mousavi, H.Z., Hosseinifar, A., Jahed, V., 2010. Removal of Cu(II) from wastewater by waste tire rubber ash. J. Serb. Chem. Soc. 75, 845–853.
Mudhoo, A., Garg, V.K., Wang, S., 2012. Removal of heavy metals by biosorption. Environ. Chem. Lett. 10, 109–117.
National Academy of Sciences (NAS), 1977. Copper. Committee on Medical and Biologic Effects of Environmental Pollutants. National Research Council, National Academy of Sciences, Washington, D.C., p. 115.
Nikiforova, T.E., Kozlov, V.A., Gagina, A.N., 2010. Sorption of copper ions by cellulose sorbents modified with a dichlorotriazine compound and polyvinylpyrrolidone. Russ. J. Appl. Chem. 83, 1774–1780.
Nriagu, J.O., 1979. The global copper cycle. Copper in the Environment. Part 1: Ecological Cycling. John Wiley, New York.
Pathania, D., Sharma, S., 2012. Effect of surfactants and electrolyte on removal and recovery of basic dye by using *Ficus carica* cellulosic fibers as biosorbent. J. Ten. Surf. Det. 49, 306–314.
Rao, M.M., Ramesh, A., Rao, G.P.C., Seshaiah, K., 2006. Removal of copper and cadmium from the aqueous solutions by activated carbon derived from *Ceiba pentandra* hulls. J. Hazard. Mater. 129, 123–129.
Rosas, J.M., Bedia, J., Rodrıguez-Mirasol, J., Cordero, T., 2009. Hemp derived activated carbon fibers by chemical activation with phosphoric acid. Fuel 88, 19–26.
Sharma, S., Pathania, D., Singh, P., 2013. Preparation, characterization and Cr (VI) adsorption behavior study of poly (acrylic acid) grafted *Ficus carica* bast fiber. Adv. Mater. Lett. 4, 271–276.
Shukla, S.R., Pai, R.S., 2005. Adsorption of Cu(II), Ni(II) and Zn(II) on dye loaded groundnut shells and sawdust. Sep. Purif. Technol. 43, 1–8.
Srivastava, S.K., Tyagi, R., 1995. Competitive adsorption of substituted phenols by activated carbon developed from the fertilizer waste slurry. Water Res. 29, 483–488.
Wang, X., Qin, Y., 2006. Removal of Ni(II), Zn(II) and Cr(VI) from aqueous solution by Alternanthera philoxeroides biomass. J. Hazard. Mater. 138, 582–588.
Wang, X.S., Tang, Y.P., Tao, S.R., 2009. Kinetics, equilibrium and thermodynamic study on removal of Cu(II) using low-cost adsorbent alligator weed. Chem. Eng. J. 148, 217–225.
Yang, R., Liu, G., Xu, X., Li, M., Zhang, J., Hao, X., 2011. Surface texture, chemistry and adsorption properties of acid blue 9 of hemp (*Cannabis sativa* L.) bast-based activated carbon fibers prepared by phosphoric acid activation. Biomass Bioenergy 35, 437–445.
Zhao, X.T., Zeng, T., Hu, Z.J., Gao, H.W., Zou, C.Y., 2012a. Modeling and mechanism of the adsorption of proton onto natural bamboo sawdust. Carbohydr. Polym. 87, 1199–1205.
Zhao, X.T., Zeng, T., Li, X.Y., Hu, Z.J., Gao, H.W., Xie, Z., 2012b. Modeling and mechanism of the adsorption of copper ion onto natural bamboo sawdust. Carbohydr. Polym. 89, 185–192.

Please cite this article in press as: Gupta, V.K. et al., Adsorptive remediation of Cu(II) and Ni(II) by microwave assisted H_3PO_4 activated carbon. Arabian Journal of Chemistry (2013), http://dx.doi.org/10.1016/j.arabjc.2013.11.006